European Journal of Radiology 166 (2023) 111004

Contents lists available at ScienceDirect

European Journal of Radiology

journal homepage: www.elsevier.com/locate/ejrad

Computed vs. film-based radiographs' contour artifacts influence diagnosis of secondary caries

Jan Christian Danz [a,*], Hans Peter Flück [a,b], Guglielmo Campus [b,c,1], Thomas Gerhard Wolf [b,d,1]

[a] Department of Orthodontics and Dentofacial Orthopedics, University of Bern, Bern, Switzerland
[b] Department of Restorative, Preventive and Pediatric Dentistry, School of Dental Medicine, University of Bern, Switzerland
[c] Department of Surgery, Microsurgery and Medicine Sciences, School of Dentistry, University of Sassari, Italy
[d] Department of Periodontology and Operative Dentistry, University Medical Center of the Johannes Gutenberg-University, Mainz, Germany

ARTICLE INFO

Keywords:
Computed radiographs
Digitized radiographs
Digital imaging
Film-based
Filter
Secondary caries

ABSTRACT

To test local grey-scale changes on dental bitewing radiographs near filling margins for image acquisition. Forty approximal preparations in caries-free amalgam filled teeth and bitewing radiographs were acquired under standardized conditions applying four techniques. Film-based analog radiographs were digitized using flat-bed scanner (FDR). Phosphor-plate computed radiographs (PCR) were directly acquired by scanning VistaScan imaging plates. Image quality was tested using Preset Filter (PF) or manually applied IntraOral Fine Filter (IF) to enhance digital images. Local changes from digital imaging processing were assessed by comparing the margin-near (MN) and margin-far (MF) zone by a multivariate repeated measurements analysis. All images were acquired with 8-bit depth (256 shades). Dentine was displayed in 79 shades for FDR and 54 shades for PCR. PF or IF locally modify bitewing radiographs by darkening marginal dentine by 8 or 29 shades, respectively. The sharpest display of the margin (shades per pixel) from dentine to filling was found for IF (26.2), followed by FDR (23.2), PF (15.3) and PCR (8.3). Computed radiography with phosphor plates generate more homogeneous images compared to flatbed-digitized film-based radiographs. The filling margin was sharpest represented with the IF filter at the detriment of an artificial darkening of the dentine near the margin of the filling. Contour artifacts by filters have the potential to confound diagnosis of secondary caries. Algorithms and filters for sensor data processing, causing local changes above 2% of the dynamic range by non-continuous mathematical functions, should only be applied with caution, manually when diagnosing and reversibly.

1. Introduction

Bitewing radiology provides best diagnostic accuracy to diagnose approximal and secondary caries, after inspection and palpation have indicated possible presence of a carious lesion or a marginal gap [11]. Analogue film-based radiographs are slowly disappearing due to the broad availability of digital techniques [24,28]. However, the use of digital intraoral images also raises questions regarding dose, image quality, artifacts, and diagnostic reliability [1,4,10,23,25,28,30]. The recognizability of image features and the details important for diagnosis must correspond to the information content of the radiographs [10,20]. Phosphor-plate computed radiographs have the advantage of a wider exposure range, generating acceptable consistent radiographs even with large variation in radiation dose [2,5,9]. Subjective image quality varies depending on the calibration of the sensor for the intended use and the image recognition and interpretation system used to produce an original image that is optimal for diagnosis, sharing and storage [14,28].

Post-processing functions and filters on the original image, such as sharpness and contrast enhancement, can be used by the diagnostician to optimize X-ray images for specific tasks [18,31]. The diagnostician intends to improve the quality of the X-ray image or to achieve higher accuracy in the assessment of diagnostic problems with the help of software technology [6]. However, misinterpretations can also lead to incorrect diagnoses and consequently incorrect therapies. Diagnostically relevant structures can be suppressed using various filters and directly lead to misinterpretations [29]. This can happen unknowingly with

* Corresponding author at: Department of Orthodontics and Dentofacial Orthopedics, School of Dental Medicine, University of Bern, Freiburgstrasse 7, CH-3010 Bern, Switzerland.
E-mail address: jan.danz@unibe.ch (J.C. Danz).

[1] These authors contributed equally.

https://doi.org/10.1016/j.ejrad.2023.111004
Received 6 June 2023; Received in revised form 17 July 2023; Accepted 20 July 2023
Available online 22 July 2023

software presets, contrast enhancement filters or sharpness filters, which can influence the X-ray image positively as well as negatively [16]. Improper post-processing of radiographs can cause a reduction in diagnostic performance [31]. In case of a marginal gap below an approximal filling, secondary caries can be diagnosed clinically, and the cavity's extension is verified on bitewing radiographs [10]. In the case of non-cavitated lesions that are only radiologically visible, the assessment of secondary caries may be more difficult [21]. Ring artifacts by mathematical algorithms used in filters were shown to occur predominantly at areas that have sharp transitions [17]. The true and precise display of the transitions between the filling and dentine is crucial for marginal caries diagnosis. Artifacts influence and complicate the diagnosis based on radiographs [4,12]. Although several studies have addressed the quality of digital radiology [8,26,27], studies on dental-anatomically correct image reproduction or artifacts by local changes by digital radiographic techniques are lacking [15]. Inhomogeneities in the filling margin area in the absence of caries or a marginal gap may lead to misinterpretations that have clinical implications for the diagnosis and treatment of secondary caries. The aim of this study is to compare the influence of four different techniques to acquire bitewing radiographs on artifacts which are seen as local differences in dentine between areas near and far from the filling margin.

2. Materials and methods

2.1. Tooth selection and preparation

Forty approximal restorations were placed in extracted human first molars, with healthy undamaged enamel and coronal dentine. Twenty premolars and twenty molars served as adjacent teeth to create a natural contact area. All teeth come from a collection of universities in Switzerland and southwestern Germany, which were made available for research purposes. The roots embedded in methyl methacrylate (ProBase Cold, Ivoclar, Vaduz, Liechtenstein). Forty Class II cavities were prepared in mesial and distal aspects. The dimensions of the Class II cavities were as follows: occlusal 1 mm reduced and mesio-distal extension of 3 mm; slot against apical 3 mm, bucco-lingual 1.5 mm and mesio-distal 1.5 mm. All prepared teeth were filled with amalgam.

2.2. Radiography

The preparations were each X-rayed using the orthoradial X-ray technique. A bitewing plastic wing was placed on the occlusion of the fixed molar and the distance guide was standardized at 3 cm. The X-ray tube was adjusted from buccal so that the examination area was fully irradiated, and a perpendicular beam path appeared on the film. This positioning device allows the standardized production of radiographs which correspond closely to clinical bitewing radiographs (Fig. 1). All radiographs were taken with equal settings: a voltage of 63 kV, a tube current of 8 mA and an exposure time of 0.200 s. Prior to image acquisition, a consistency test was conducted. Analogue images were captured on Insight super Poly-Soft size 2 (Carestrem Health Inc., Le Perreux-sur-Marne, France) films with a PLANMECA intra (Planmeca Oy, Helsinki, Finland) x-ray tube. Subsequently, the films were processed semi-automatically (PerioMat, Dürr Dental SE, Bietigheim-Bissingen, Germany, www.duerrdental.com). Computed images were acquired using a BELRAY Model 096 X-ray unit (Takara Belmont Corporation, Osaka, Japan) and by scanning VistaScan imaging plates Plus 2+ (Dürr Dental SE and VistaScan mini-View, Germany, www.duerrdental.com).

2.3. Radiologic imaging and post-processing techniques

Four techniques for radiologic display of filling margins were used (Fig. 2): In the film-based and digitized radiography technique (FDR), the films were digitized by 8-bit 1200 DPI scanning with EPSON Expression 1680 Pro flatbed scanner (Seiko Epson Corporation, Suwa, Nagano, Japan) and exported as.JPG format. The phosphor-plate computed radiographs (PCR) were exported with all filters removed. In the preset filter group (PF), the filter for image enhancement which is automatically applied by the software has been kept. In the IntraOral Fine filter technique (IF) an additional post-processing filter from DBSWIN was applied. All radiographs based on phosphor-plates were exported 1272 DPI resolution from DBSWIN imaging software (Dürr Dental SE, Germany, www.duerrdental.com) as .PG format. All images were exported in 256 grey-scales (8-bit dept).

2.4. Measurements

Grey levels in an area of 100 pixels around the filling margin were measured using ImageJ 1.53 (National Institutes of Health, Rockville Pike, Bethesda, Maryland, USA) by one observer. A fourfold magnification was used to draw a measurement line perpendicular to the filling margin with the filling margin between pixel 50 and 51. The double measurement of the samples took place five days after the first measurement.

2.5. Area of interest

The filling margin is represented in a radiographic image as a

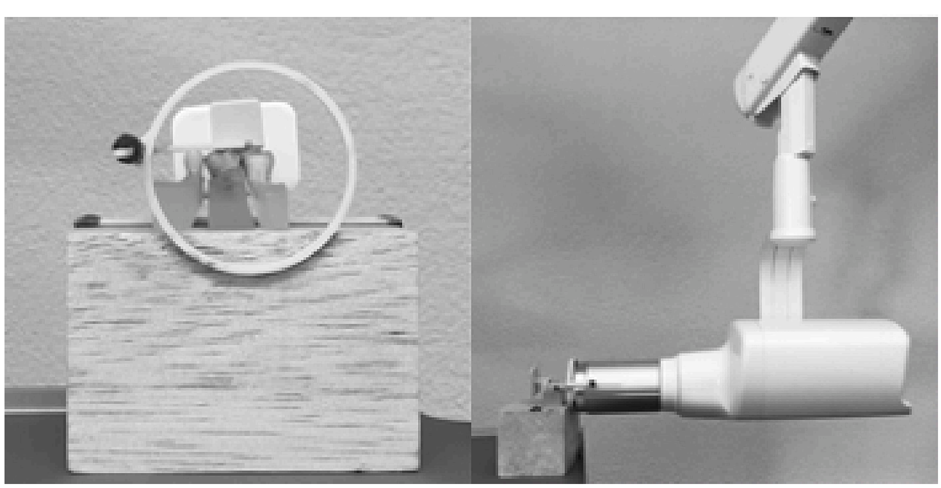

Fig. 1. The mounting device ensures standardized bitewing radiographs with perpendicular alignment of the tube to the film. The fillings were put in contact with adjacent teeth.

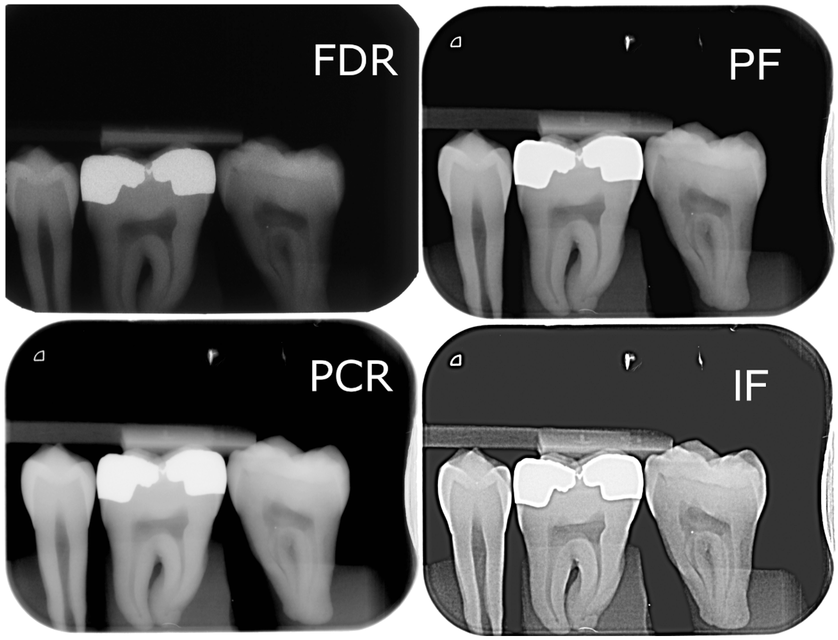

Fig. 2. Bitewing radiographs of an average specimen acquired with analogue film-based technique (FDR) or digital computed technique (PCR) and with applied preset filter (PF) or IntraOral Fine filter (IF). The dynamic range between amalgam and dentine was largest for FDR, smallest for PCR and locally altered at filling margins by PF and IF creating bright and dark contour artifacts.

transition zone, where the median grey value of dentine changes gradually to the median value of the filling material. The width of the transition zone was defined from the 10 percentiles of amalgam to the 90 percentiles of dentine gray values. Based on the assumption that the filling margin lies exactly in the middle between bright (filling) and dark (dentine) pixels, the inversion point was calculated as the median value of the grey levels for each group. A margin-near (MN, pixel 53–57) and a margin-far (MF, pixel 73–77) zone was defined for comparison of local changes and to compare them between techniques (Fig. 3).

2.6. Data analysis and measurement error

Bland Altman analysis was calculated using GraphPad Prism 9 (GraphPad Software, Boston, MA, USA) to estimate intervals of agreements between double measurements. Data was imported to STATA 12.0 (StatCorp, College Station, Texas, USA) for descriptive statistical analysis. Local changes from digital imaging processing were assessed by comparing margin-near and the margin-far zone by a multivariate repeated measurements analysis using technique and zone as random coefficients with intercepts. Residuals were calculated and plotted.

3. Results

The median grey value of all pixels is for FDR 123 (between pixel 50/51), for PCR 220 (between pixel 49 and 50), for PF 180 (between pixel 49 and 50) and for IF 187 (between pixel 49 and 50). Depending on the technique, dentine and amalgam are mapped at different locations on the grey scale (Table 1). In addition, also the difference between median grey value of amalgam and dentine varies and is for FDR 116 shades, for PCR 41 shades, for PF 77 shades and for IF 79 shades. The transition zone between amalgam and dentine is for FDR 5 pixels (slope 23.2 shades per pixel), for PCR 5 pixels (slope 8.3 shades per pixel), for PF 5

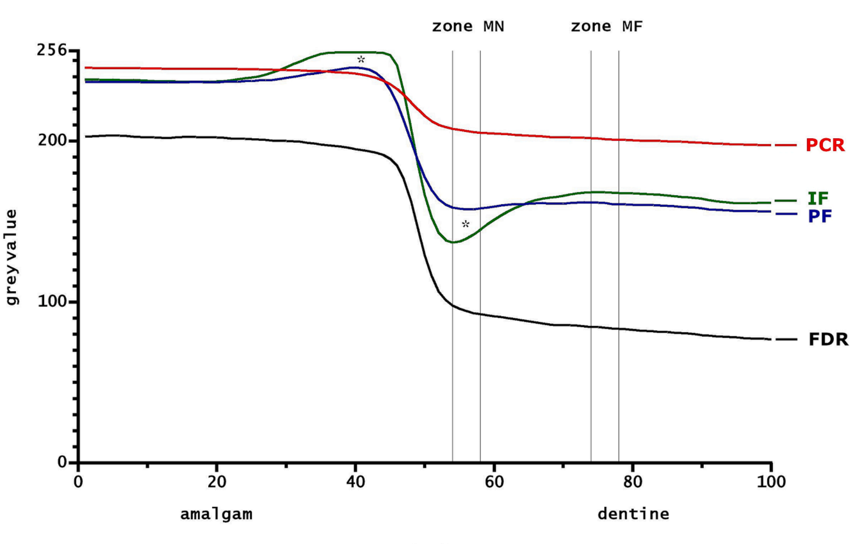

Fig. 3. The mean grey values at each pixel from amalgam to dentine are shown for analogue film-based technique (FDR), digital computed technique (PCR), preset filter (PF) and IntraOral Fine filter (IF). The dentine at margin-near zone near (MN) was compared to the zone further away (MF). It is expected that the grey values decrease slightly from near the margin (MN) to far from the margin (MF) of the filling, as less tooth substance is penetrated towards the apex. Artifacts (*) were found for PF and IF near the filling margin in dentine and in amalgam.

Table 1
Descriptive table of grey values for analogue film-based technique (FDR), digital computed technique (PCR), Preset filter group (PF) and the IntrOral Fine filter group (IF).

Technique	Tissue	Grey value Median	Grey value 10% Quantile	Grey value 90% Quantile
FDR	Amalgam	200	183	207
	Dentine	84	68	106
PCR	Amalgam	244	234	247
	Dentine	202	188	214
PF	Amalgam	237	230	244
	Dentine	160	147	173
IF	Amalgam	239	234	255
	Dentine	160	141	178

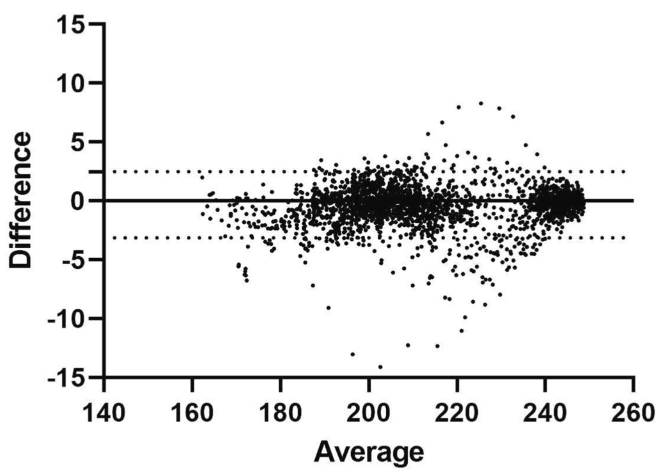

Fig. 4. The Bland-Altman plot shows non-significant bias of −0.32 grey values between double measurements with a 95% limits of agreement from −3.13 to 2.48. One dotted arc upwards and one downwards could be a mismeasurement of two specimen, e.g. measured wrong image in one of the double measurements. No measurements were excluded.

pixels (slope 15.3 shades per pixel) and for IF 3 pixels (slope 26.2 shades per pixel) wide. The mean grey values at each pixel from amalgam to dentine are shown in Fig. 3. Bland Altman comparison of double measurements resulted in non-significant bias of −0.32 Grey value and 95% limits of agreement from −3.13 to 2.48 (Fig. 4).

3.1. *Display of dentine: Film-based and digitized radiographs vs. phosphor-plate computed radiographs*

Mean grey values of FDR and PCR were significantly different to all other groups ($p < 0.01$). The range of shades in dentine was 79 for FDR and 54 for PCR. The dentine darkens in FDR by 12 shades ($p < 0.01$) and in PCR by 5 shades ($p < 0.01$)) from zone MN to zone MF. Dentine of FDR is displayed 110 shades darker at zone MN and 117 shades darker at zone MF than dentine of PCR. The darker display of dentine from MN to MF is not parallel between FDR an PCR. The grey value darkens by 7 shades more in FDR than in PCR ($p < 0.01$) from zone MN to zone MF.

3.2. *Display of dentine: Preset Filter*

The application of PF on digital radiographs decreases overall brightness by 49 shades at zone MN ($p < 0.01$) and by 40 shades at zone MF ($p < 0.01$). The range of shades in dentine was 59 for PF. The dentine in PF is 3 shades ($p < 0.01$) darker at zone MN than at zone MF, whereas in PCR it was the opposite. The change between zone MN to zone MF is 8 shades different when comparing PF with PCR ($p < 0.01$).

3.3. *Display of dentine: IntraOral Fine filter*

In IF, the darkening is 68 shades at MN ($p < 0.01$) and 33 shades at MF ($p < 0.01$) when com paring to PCR. The range of shades of dentine is 122 for IF. The dentine is modified by IF in the amount of 29 shades ($p < 0.01$) brighter from MN to MF. The darkening at MN is 9.7-fold higher in IF than in PF ($p < 0.01$).

4. Discussion

Bite-wing radiographs of caries-free restorations obtained by digitalized analog films, by phosphor-plate computed radiography and by two filters were compared regarding changes of the grey value of dentine near the filling margin and dentine far from the filling margin. The observed range of 117 out of a total of 256 shades of grey for dentine varies depending on the amount of irradiated tissue and on the technique. The diagnosis is therefore based on the relative comparison between areas in the radiograph and the shape or difference in brightness expected by the dentist. An influence of the dose on the image quality or brightness was avoided in this study, as the acquisition parameters were the same for all methods [1,23]. A limitation of this study is that it does not directly measure the impact of the algorithms on the specificity and sensitivity of caries diagnosis because only caries-free teeth were used.

Alongside the resolution and the used grayscale range for the tissue of interest, the dental-anatomically correct image reproduction is particularly important for the quality in radiology.

Images generated by PCR were found to be more homogeneous and the range of shades was lowest with 54 for dentine. Although the chemical processing of the films (temperature, time, consumption of chemicals) and consistent settings during digitalization with a scanner, the numerous steps could have resulted in 79 shades wider range of for dentine (Fig. 5). The reduction in image quality by digitalization of film-based radiographs, especially in darker image areas can partially explain the differences between FDR and PCR [7,22]. Even though the dynamic range of FDR is highest, the higher average brightness of the tissue dentine in PCR could be an advantage, since bright images are less sensitive to ambient light for diagnosis [3]. Applying PF and IF filter to PCR increased the range of greyscale from 54 for dentine to 59 and 122, respectively. As these changes by filters are not evenly distributed in marginal and near-marginal dentine, artifacts near the contour of the filling margin appear, which are likely to influence the diagnosis of

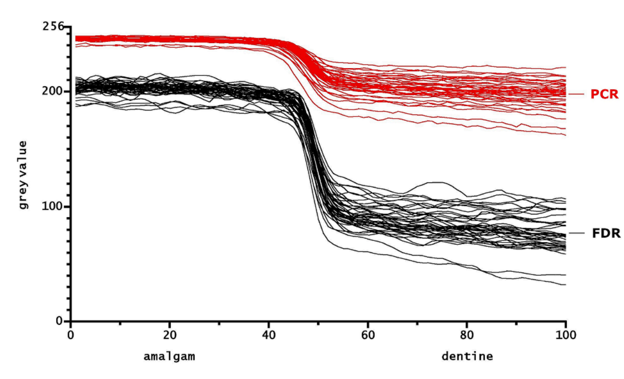

Fig. 5. For each of the forty fillings, a red line represents the digital computed radiographs (PCR) and a black line the analogue film-based radiographs (FDR) for radiographic imaging. Amalgam and dentine of the analogue technique is represented in a darker band of grey values with a larger range. The step in grey values between amalgam and dentin is larger for the analogue technique than for the digital technique. (For interpretation of the references to colour in this figure legend, the reader is referred to the web version of this article.)

secondary caries. The difference of 8 shades caused by filter PF is detectable by the human eye and clinically relevant, but not obvious without comparison to the original digital image since the pixels are changed gradually over a larger distance. In IF, the effect of the filters to increase the contrast in the marginal area was 9.7 times greater and well visible in the dentine as dark contour artifacts and in the filling material as a white contour artifact. The same artifacts can also be found close to filling as brighter spots from pixels 36 to 45, where modifications by the filter have exceeded the maximum brightness of 256 shades (Fig. 3). Therefore, PF and IF filters seem to locally modify the image near the margin of the filling creating artificial darkening or brightening of specific areas. The occurrence of artifacts was solely measured between dentin and fully radio-opaque restorative material. It can be expected that algortihms cause less artifacts at tissue transitions with a smaller difference in radioopacity. Also ring artifacts are caused by filters, which can lead to image modification that potentially distort diagnostics [12].

A short and steep transition zone between different tissues is a subjective indicator for image quality (Fig. 3). The transition zone between dentine and filling was narrowest (3 pixels) and steepest (26.2 shades per pixels) after application of IF filter, resulting in the subjectively sharpest image for IF. All other transition zones were 5 pixels wide with a slope (shades per pixel) of 23.2 for FDR, of 15.3 for PF and 8.3 for PCR.

The computed image is different from the film-based image with changes that cannot be explained by changes in brightness, contrast, or other linear calculations alone. Human visual perception seems to function well from 64 levels of grey but can differentiate up to 900 shades of grey under optimal conditions [13,19]. We consider a local change of 5 grayscales (2% of dynamic range of the image) clinically significant. The ability by computed image acquisition to adjust grey value of a tissue, e.g., dentine, independently of the dose offers more possibilities in image standardization [26]. The processing of the sensor data by PCR was found herein to produce more uniform images than with FDR. Histograms of a FDR gamma brightened image and a PCR image have in common that the darkest gray levels are unused (Fig. 6). Brightening the images by placing gray scale ranges of important tissues, in ranges with best human visual perception, may improve the diagnosis. A combination of logarithmic image transformation (gamma) and square root transformation with extension of the range to the maximum (equalization) could improve visibility of important tissues without artifacts and without information loss larger than 2% by pixel saturation. The ability to create consistently uniform images with computed technology is an advantage over analogue technology among lower dose, faster image acquisition, fewer errors and easier storage or communication [28]. However, mathematical functions used in digital computed radiology to process the sensor image and for post-processing should be disclosed so that the diagnostician is aware of the possible occurrence of artifacts. When using artificial intelligence for diagnosis, it will always be necessary that the diagnosis is verified by a human. The two filters tested herein caused local changes such as darkening of dentine at the filling margin. Preset algorithms used for transformation of sensor data to create the original image and manually added algorithms for image enhancement during diagnosis should be tested for possible artifacts which can interfere with diagnosis and published before clinical application.

5. Conclusions

The digital transformation of sensor data into a greyscale image results in a more homogeneous image than film-based acquisition. We consider algorithms in computed radiography used to adapt sensor data optimally for on-screen viewing, which cause $<$ 2% local changes in grayscale values, to be clinically acceptable. All filters causing larger local changes should only be applicable manually and reversibly during diagnosis. Future research should focus on how to improve sensor data for human visual perception (gamma and tissue equalization), preferably with minimal data loss and without the occurrence of artifacts, and how diagnosis is affected by the use of algorithms including artificial intelligence.

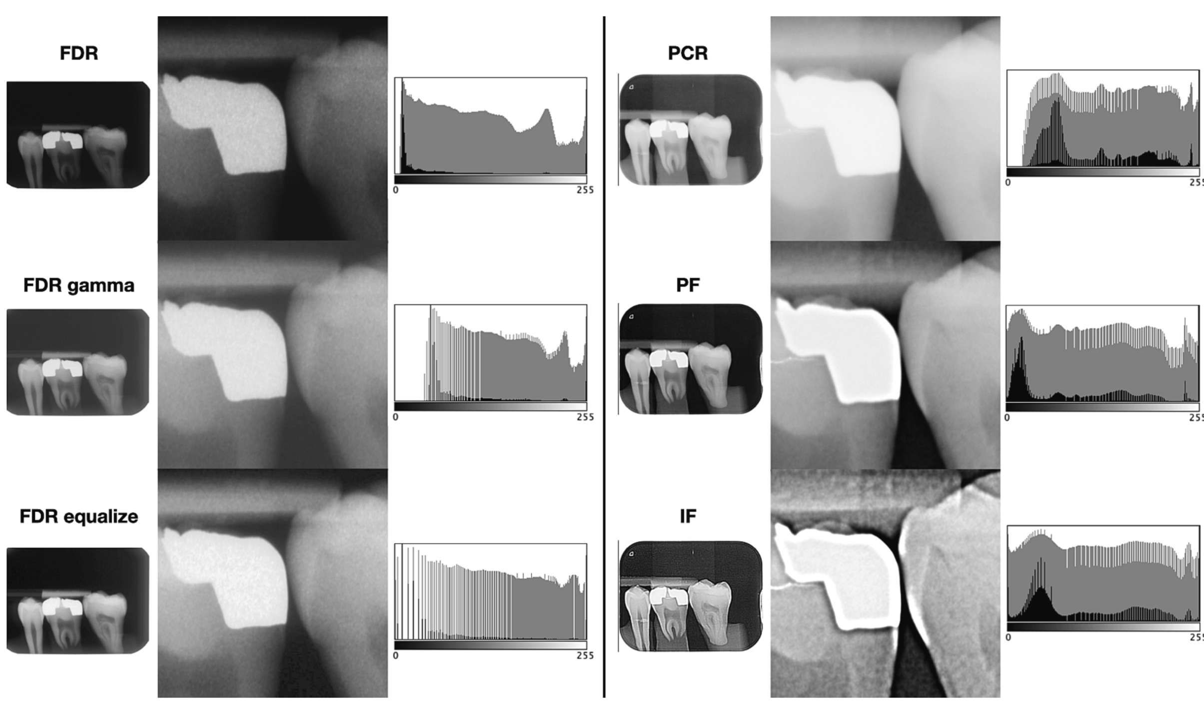

Fig. 6. Magnifications, histograms (black) and logarithmic histograms (grey) of specimen number 2. The film-based digitized radiograph (FDR) is the darkest image with a mean grayvalue of 44 ± 58, followed by FDR with equalized histogram 76 ± 71, preset filter (PF) 80 ± 77, FDR with gamma filter 90 ± 55, IntraOral Fine Filter (IF) 101 ± 76 and phosphor-plate computed radiographs (PCR) 121 ± 68. PF and IF showed not only an artificial darkening in the dentin near the filling but also a gap formation between the teeth (enlargement of opaque material or shrinkage of radiolucent tissues) and a saturation of the pixels to white in the enamel area.

Credit authorship contribution statement

Jan Christian Danz: Conceptualization, Methodology, Software, Validation, Formal analysis, Investigation, Data curation, Writing – original draft, Writing – review & editing, Visualization, Supervision, Project administration. **Hans Peter Flück:** Methodology, Software, Investigation, Data curation, Writing – original draft. **Guglielmo Campus:** Conceptualization, Validation, Formal analysis, Data curation, Writing – review & editing, Supervision, Project administration. **Thomas Gerhard Wolf:** Conceptualization, Validation, Data curation, Writing – review & editing, Supervision, Project administration.

Declaration of Competing Interest

The authors declare that they have no known competing financial interests or personal relationships that could have appeared to influence the work reported in this paper.

Data availability

The data that support the findings of this study are available on request from the corresponding author.

References

[1] C. Aziman, K. Hellén-Halme, X.-Q. Shi, A comparative study on image quality of two digital intraoral sensors, Dentomaxillof. Radiol. 48 (2019) 20190063, https://doi.org/10.1259/dmfr.20190063.

[2] W.E.R. Berkhout, D.A. Beuger, G.C.H. Sanderink, P.F. van der Stelt, The dynamic range of digital radiographic systems: Dose reduction or risk of overexposure? Dento Maxillo Facial Radiol. 33 (2004) 1–5, https://doi.org/10.1259/dmfr/40677472.

[3] A.S. Chawla, E. Samei, Ambient illumination revisited: a new adaptation-based approach for optimizing medical imaging reading environments, Med. Phys. 34 (2007) 81–90, https://doi.org/10.1118/1.2402583.

[4] W.T. Drost, D.J. Reese, W.J. Hornof, Digital radiography artifacts, Vet. Radiol. Ultrasound Off. J. Am. Coll. Vet. Radiol. Int. Vet. Radiol. Assoc. 49 (2008) 48–56, https://doi.org/10.1111/j.1740-8261.2007.00334.x.

[5] A.G. Farman, T.T. Farman, A comparison of 18 different x-ray detectors currently used in dentistry, Oral Surg. Oral Med. Oral Pathol. Oral Radiol. Endod. 99 (2005) 485–489, https://doi.org/10.1016/j.tripleo.2004.04.002.

[6] T. Gillespy, A.H. Rowberg, Displaying radiologic images on personal computers: image processing and analysis, J. Digit. Imag. 7 (1994) 51–60, https://doi.org/10.1007/BF03168422.

[7] N.J. Hangiandreou, T.J. O'Connor, J.P. Felmlee, An evaluation of the signal and noise characteristics of four CCD-based film digitizers, Med. Phys. 25 (1998) 2020–2026, https://doi.org/10.1118/1.598390.

[8] R.C. Hoogeveen, S. Ouchene, W. Berkhout, Diagnostic image quality of hand-held and wall-mounted X-ray devices in bitewing radiography: a non-inferiority clinical trial, Dento Maxillo Facial Radiol. 50 (2021) 20200471, https://doi.org/10.1259/dmfr.20200471.

[9] W. Huda, L.N. Rill, D.K. Benn, J.C. Pettigrew, Comparison of a photostimulable phosphor system with film for dental radiology, Oral Surg. Oral Med. Oral Pathol. Oral Radiol. Endod. 83 (1997) 725–731, https://doi.org/10.1016/s1079-2104(97)90327-9.

[10] M. Hyvönen, A. Jaakkola, T. Tanner, J. Päkkilä, A. Kämppi, P. Patinen, L. Tjäderhane, A. Sipola, S. Huumonen, V. Anttonen, Quality and findings of bitewing radiographs among twenty-year-old conscripts in Finland, Int. J. Dent. 2021 (2021) 8894917, https://doi.org/10.1155/2021/8894917.

[11] M. Janjic Rankovic, S. Kapor, Y. Khazaei, A. Crispin, I. Schüler, F. Krause, K. Ekstrand, S. Michou, F. Eggmann, A. Lussi, M.-C. Huysmans, K. Neuhaus, J. Kühnisch, Systematic review and meta-analysis of diagnostic studies of proximal surface caries, Clin. Oral Investig. 25 (2021) 6069–6079, https://doi.org/10.1007/s00784-021-04113-1.

[12] T.L. Ji, M.K. Sundareshan, H. Roehrig, Adaptive image contrast enhancement based on human visual properties, IEEE Trans. Med. Imag. 13 (1994) 573–586, https://doi.org/10.1109/42.363111.

[13] T. Kimpe, T. Tuytschaever, Increasing the number of gray shades in medical display systems–how much is enough? J. Digit. Imag. 20 (2007) 422–432, https://doi.org/10.1007/s10278-006-1052-3.

[14] H. Kitagawa, A.G. Farman, J.P. Scheetz, W.P. Brown, J. Lewis, M. Benefiel, K. Kuroyanagi, Comparison of three intra-oral storage phosphor systems using subjective image quality, Dento Maxillo Facial Radiol. 29 (2000) 272–276, https://doi.org/10.1038/sj/dmfr/4600532.

[15] M.W. Kusk, J.M. Jensen, E.H. Gram, J. Nielsen, H. Precht, Anode heel effect: does it impact image quality in digital radiography? A systematic literature review, Radiogr. Lond. Engl. 1995 (27) (2021) 976–981, https://doi.org/10.1016/j.radi.2021.02.014.

[16] G. Li, G.C.H. Sanderink, W.E.R. Berkhout, K. Syriopoulos, P.F. van der Stelt, Detection of proximal caries in vitro using standard and task-specific enhanced images from a storage phosphor plate system, Caries Res. 41 (2007) 231–234, https://doi.org/10.1159/000099324.

[17] Y. Li, L. Sharan, E.H. Adelson, Compressing and companding high dynamic range images with subband architectures, ACM Trans. Graph. 24 (2005) 836–844, https://doi.org/10.1145/1073204.1073271.

[18] T.H. Lin, T. Kao, Adaptive local contrast enhancement method for medical images displayed on a video monitor, Med. Eng. Phys. 22 (2000) 79–87, https://doi.org/10.1016/s1350-4533(00)00014-x.

[19] M. Oberholzer, M. Ostreicher, H. Christen, M. Brühlmann, Methods in quantitative image analysis, Histochem. Cell Biol. 105 (1996) 333–355, https://doi.org/10.1007/BF01463655.

[20] F.A. Pasler, H. Visser, Taschenatlas der Zahnärztlichen Radiologie, Georg Thieme Verlag, 2003.

[21] M.P. Rudolphy, Y. Gorter, C. van Loveren, J.P. van Amerongen, Validity of radiographs for diagnosis of secondary caries in teeth with class II amalgam restorations in vitro, Caries Res. 31 (1997) 24–29, https://doi.org/10.1159/000262369.

[22] R.K.W. Schulze, S.T.R. Rosing, B. D'Hoedt, Contrast perception in digitized panoramic radiographs compared with their film-based origin, Oral Surg. Oral Med. Oral Pathol. Oral Radiol. Endod. 94 (2002) 388–394, https://doi.org/10.1067/moe.2002.126450.

[23] C. Steffensen, G. Trypis, G.T.W. Mander, Z. Munn, Optimisation of radiographic acquisition parameters for direct digital radiography: a systematic review, Radiogr. Lond. Engl. 1995 (27) (2021) 663–672, https://doi.org/10.1016/j.radi.2020.08.012.

[24] T. Stodt, T. Attin, [Bitewing examinations as a part of preventive dentistry–a review], Schweiz. Monatsschrift Zahnmed. Rev. Mens. Suisse Odonto-Stomatol. Riv. Mens. Svizzera Odontol. E Stomatol. 114 (2004) 882–889.

[25] I.A. Tsalafoutas, S. AlKhazzam, V. Tsapaki, H. AlNaemi, M.H. Kharita, Digital radiography image quality evaluation using various phantoms and software, J. Appl. Clin. Med. Phys. 23 (2022) e13823.

[26] M. Uffmann, C. Schaefer-Prokop, Digital radiography: the balance between image quality and required radiation dose, Eur. J. Radiol. 72 (2009) 202–208, https://doi.org/10.1016/j.ejrad.2009.05.060.

[27] T. Ulusu, H. Bodur, M.E. Odabaş, In vitro comparison of digital and conventional bitewing radiographs for the detection of approximal caries in primary teeth exposed and viewed by a new wireless handheld unit, Dentomaxillof. Radiol. 39 (2010) 91, https://doi.org/10.1259/dmfr/15182314.

[28] A. Wenzel, A. Møystad, Work flow with digital intraoral radiography: a systematic review, Acta Odontol. Scand. 68 (2010) 106–114, https://doi.org/10.3109/00016350903514426.

[29] S.C. White, M.J. Pharoah, Oral Radiology - E-book: Principles and Interpretation, Elsevier Health Sciences, 2014.

[30] T.G. Wolf, F. Fischer, R.K.W. Schulze, Correlation of objective image quality and working length measurements in different CBCT machines: an ex vivo study, Sci. Rep. 10 (2020) 19414, https://doi.org/10.1038/s41598-020-76424-4.

[31] S. Yalcinkaya, A. Künzel, R. Willers, M. Thoms, J. Becker, Subjective image quality of digitally filtered radiographs acquired by the Dürr Vistascan system compared with conventional radiographs, Oral Surg. Oral Med. Oral Pathol. Oral Radiol. Endod. 101 (2006) 643–651, https://doi.org/10.1016/j.tripleo.2005.08.003.